

Incoherent mesoscopic hole tunneling through barrier states in p -type $\text{Al}_x\text{Ga}_{1-x}\text{As}$ capacitors

T. W. Hickmott

IBM Research Division, Thomas J. Watson Research Center, Yorktown Heights, New York 10598

(Received 3 February 1992; revised manuscript received 28 May 1992)

Hole tunneling from an accumulation layer in single-barrier p^- -type GaAs-undoped $\text{Al}_x\text{Ga}_{1-x}\text{As}$ - p^+ -type GaAs capacitors results in complex current-voltage (I - V) characteristics. At low bias, in the direct tunneling regime, several reproducible voltage-controlled negative resistance regions can occur. I - V curves for a given sample are reproducible while I - V curves for nominally identical samples vary from sample to sample. I - V curves are exponential in voltage with fluctuations in $\ln(dJ/dV) \sim 1$. Detailed structure in curves of $d(\ln J)/dV$ versus voltage is temperature dependent for $T < 70$ K. At 1.7 K structure in derivative curves is independent of magnetic field. The observed behavior is consistent with the models reviewed by Raikh and Ruzin for incoherent mesoscopic tunneling through states in a randomly nonuniform barrier. The origin of the states in the nominally undoped $\text{Al}_x\text{Ga}_{1-x}\text{As}$ barrier is probably Be diffusing from regions of high doping sample growth.

I. INTRODUCTION

Tunneling in metal-insulator-metal (MIM) or semiconductor-insulator-semiconductor (SIS) structures is the primary conduction mechanism at low temperatures when the insulator layer is thin, the fields are high, or the metal-insulator or semiconductor-insulator barrier heights are small. The ideal structure to study tunneling in solids is one in which the source of carriers, the dielectric insulator, and the biasing electrode are lattice-matched single-crystal solids. Single-barrier n -type $\text{Al}_x\text{Ga}_{1-x}\text{As}$ capacitors which consist of an n^- -type GaAs substrate, an undoped $\text{Al}_x\text{Ga}_{1-x}\text{As}$ dielectric, and an n^+ -type GaAs gate closely approximate the ideal.¹ A variety of phenomena have been found to produce structure in current-voltage (I - V) and capacitance-voltage (C - V) curves of n -type $\text{Al}_x\text{Ga}_{1-x}\text{As}$ capacitors. Oscillatory structure with a period of 36 mV due to interaction of tunneling electrons with LO phonons in GaAs has been observed when electrons tunnel from an n^+ -type GaAs gate into the depletion region of an n^- -type GaAs substrate of an n -type $\text{Al}_x\text{Ga}_{1-x}\text{As}$ capacitor.²⁻⁵ In some cases, a magnetic field B was required to observe phonon oscillations,^{2,3} in other cases they were observed when $B=0$.⁴ An accumulation layer forms on the n^- -type GaAs substrate of an n -type $\text{Al}_x\text{Ga}_{1-x}\text{As}$ capacitor when the gate voltage V_G is positive. Resonant Fowler-Nordheim tunneling of electrons from an accumulation layer can modulate I - V characteristics when $B=0$ if the $\text{Al}_x\text{Ga}_{1-x}\text{As}$ layer is of the proper thickness.^{6,7} A magnetic field perpendicular to the two-dimensional electron gas (2DEG) of the accumulation layer quantizes the density of states into Landau levels. Structure in I - V and C - V curves reflects the properties of such Landau levels.^{8,9} When a magnetic field is parallel to the sample, structure occurs in I - V curves due to electron tunneling into magnetoelectric skipping orbits at the $\text{Al}_x\text{Ga}_{1-x}\text{As}/n^+$ -type GaAs interface.¹⁰⁻¹²

Hole tunneling in p -type $\text{Al}_x\text{Ga}_{1-x}\text{As}$ capacitors has

been less studied than electron tunneling. Recent work shows that hole tunneling from an accumulation layer in single-barrier p -type $\text{Al}_x\text{Ga}_{1-x}\text{As}$ capacitors produces remarkably complex structure in the I - V characteristics.^{13,14} When holes tunnel into a depletion layer in p^- -type GaAs, structure is observed, when the bias voltage exceeds 0.4 V, which has a periodicity of 39 mV, approximately that of the LO phonon energy of GaAs.^{14,15} Additional complex structure occurs for lower bias voltages. In this paper we present more extensive data on hole tunneling from an accumulation layer in single-barrier p -type $\text{Al}_x\text{Ga}_{1-x}\text{As}$ capacitors, and show that structure in I - V curves is in accord with models for tunneling through localized states in the undoped $\text{Al}_x\text{Ga}_{1-x}\text{As}$ dielectric.

It has been known for many years that states in the dielectric of a MIM structure can provide a channel for increased tunneling current over that which would be observed if such states were not present.¹⁶ Examples of structure in current-voltage (I - V) curves where such states have been observed are the observations of structure due to organic molecules in tunnel barriers,¹⁷ structure in I - V curves of metal-oxide-semiconductor (MOS) capacitors due to localized states caused by drifting of sodium ions in SiO_2 ,¹⁸ tunneling through localized states in amorphous silicon that serves as part of the dielectric of a MIM capacitor,^{19,20} or tunneling through electronic states in field-effect transistors.²¹⁻²⁵ From the point of view of interpreting experiments it is difficult to tell whether unusual structure in I - V characteristics of tunnel structures is due to localized states in the dielectric, to shorts, to "formed" channels through which conduction occurs,²⁶ or to some other mechanism. Raikh and Ruzin (RR) have recently reviewed work on transmittancy fluctuations in randomly nonuniform barriers.²⁷ They discuss a variety of models in which there are "punctures" or "perforations"²⁸ that are responsible for irregular conduction characteristics in mesoscopic structures, including the model of electron transmission through a dielectric barrier in MIM structures.²⁹⁻³¹ For samples of large

but finite area, the conductivity of a typical sample is determined by a few punctures of highest transmittancy in the sample. RR derive general expressions for determining the distribution functions for punctures by measuring the conductivity of a large number of samples of different areas. Such a distribution of states has been measured for gated field-effect transistor (FET) structures,²⁵ but it has not been possible to determine the distribution in single-barrier structures. RR show that if the local transmittancy of a barrier is affected exponentially strongly by an external factor F , then a distribution function for punctures can be obtained from a single sample. Their model has four consequences. First, I - V characteristics of each sample are reproducible but the dependence of conductivity on F varies between different samples that are nominally identical. Second, the conductance of different samples fluctuates around the average value, as shown schematically in Fig. 1(b), which is taken from Raikh and Ruzin.^{27,31} Fluctuations are of the order of 1 in the natural logarithm of conductance, σ . The parameter F_C in Fig. 1(b) is the correlation field for fluctuations. Third, as temperature increases, fluctuations in conductance broaden and eventually disappear. Fourth, in contrast to those mesoscopic phenomena in which conductance fluctuations arise from interference of electrons that take opposite paths around a closed loop of scatterers, fluctuations due to incoherent mesoscopic phenomena are nearly independent of magnetic field applied to a sample. Electron or hole tunneling in SIS, MIM, or MOS capacitors is exponentially dependent on field (or volt-

age), and is thus suitable for applying the model of Raikh and Ruzin.

The models discussed by RR are all couched in terms of electron tunneling or electron conduction. No results have been reported for n -type $\text{Al}_x\text{Ga}_{1-x}\text{As}$ capacitors in which structure in I - V characteristics is determined by tunneling of electrons from an accumulation layer through states or punctures in the $\text{Al}_x\text{Ga}_{1-x}\text{As}$ dielectric. In the present paper we show that hole tunneling from an accumulation layer in p -type $\text{Al}_x\text{Ga}_{1-x}\text{As}$ capacitors fits the criteria given by RR for tunneling through "punctures" or localized states in the $\text{Al}_x\text{Ga}_{1-x}\text{As}$ dielectric that are exponentially sparse but have an exponentially enhanced transmittancy.

II. EXPERIMENT

A. Sample preparation

Figure 1(a) shows a schematic energy-band diagram of the valence bands of the p -type $\text{Al}_x\text{Ga}_{1-x}\text{As}$ capacitors used to study hole tunneling. The heterostructures were grown by molecular-beam epitaxy (MBE) on a heavily p^+ -doped $\langle 100 \rangle$ -oriented GaAs wafer. They consist of a heavily doped p^+ -type GaAs buffer layer ~ 200 nm thick, a p^- -type GaAs substrate layer ~ 600 nm thick with doping $N_S \sim 6 \times 10^{14} \text{ cm}^{-3}$, an undoped $\text{Al}_{0.5}\text{Ga}_{0.5}\text{As}$ layer ~ 20 nm thick, and a p^+ -type GaAs gate layer ~ 300 nm thick with doping $N_G \sim 8 \times 10^{17} \text{ cm}^{-3}$ which was increased to $\sim 10^{19} \text{ cm}^{-3}$ at the outer surface for better ohmic contact. Beryllium is the p -type dopant. An undoped GaAs layer ~ 3 nm thick was grown on each side of the $\text{Al}_{0.5}\text{Ga}_{0.5}\text{As}$ layer which is the dielectric of the SIS capacitor. After sample growth ohmic Ag-Zn contacts were made to the p^+ -type GaAs wafer and to the p^+ -type GaAs gate. Evaporated gold films were used as an etch mask to form SIS capacitors. Samples were mounted on TO-5 headers with Ag epoxy for low-temperature measurements. Procedures for measuring I - V , capacitance-voltage (C - V), and conductance-voltage (G - V) curves have been described.^{1,8,12,32}

B. Hole accumulation layers

When the p^+ gate of a p -type $\text{Al}_x\text{Ga}_{1-x}\text{As}$ capacitor is biased negatively, a hole accumulation layer forms on the p^- -type GaAs substrate as shown schematically in the electron energy-band diagram of Fig. 1(a). E_V and E_F show the valence band and Fermi level as a function of distance. V_G is the applied voltage, V_I is the voltage across the insulator, ψ_S is the band bending in the substrate, and ψ_G is the band bending in the gate. q is the electron charge, w is the $\text{Al}_x\text{Ga}_{1-x}\text{As}$ thickness, d is the thickness of the p^- -type GaAs substrate, ϕ_G is the barrier height at the $\text{Al}_x\text{Ga}_{1-x}\text{As}/p^+$ -type GaAs interface, and ϕ_S is the barrier height at the p^- -type GaAs/ $\text{Al}_x\text{Ga}_{1-x}\text{As}$ interface. E_A indicates the approximate position of the Be acceptor in $\text{Al}_{0.5}\text{Ga}_{0.5}\text{As}$.

The valence-band structure of GaAs is complex.³³⁻³⁷ For bulk GaAs at $k=0$ there are degenerate heavy-hole

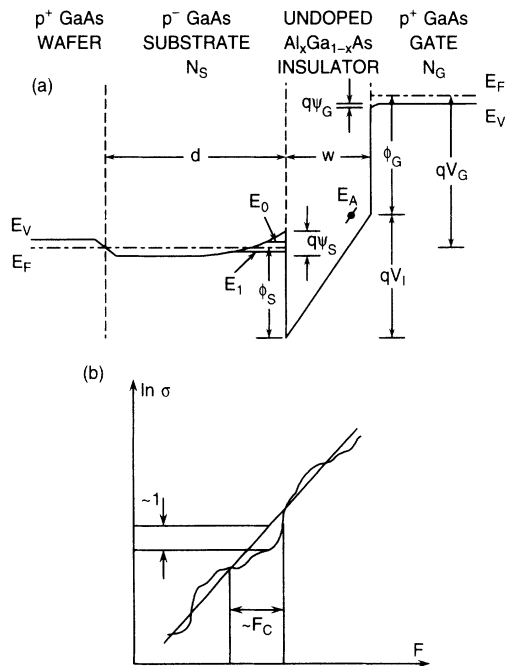


FIG. 1. (a) Schematic energy band diagram for p^- -type GaAs-undoped $\text{Al}_x\text{Ga}_{1-x}\text{As}$ - p^+ -type GaAs($\text{Al}_x\text{Ga}_{1-x}\text{As}$) capacitor biased into accumulation. (b) Schematic representation of random fluctuations of $\ln \sigma$ during change of external field F . From Raikh and Ruzin, Ref. 31.

and light-hole bands, and a split-off band which can be ignored. In an accumulation or inversion layer the light-hole band splits off from the heavy-hole band at $k=0$ due to differences in effective mass of the two bands. If $k \neq 0$, the twofold degenerate heavy- and light-hole bands are further split by loss of inversion symmetry, so that there are four hole bands in an accumulation layer whose relative separation varies as N_H , the hole density in the accumulation layer, increases. In an accumulation layer each of the hole bands is quantized in the direction perpendicular to the $\text{Al}_x\text{Ga}_{1-x}\text{As}$ barrier; it has a minimum energy, as shown schematically for two bands in Fig. 1(a), E_0 and E_1 . In a hole accumulation layer the ground state for holes is a heavy-hole level perpendicular to the interface, which is highest in energy on an electron energy-band diagram such as in Fig. 1(a). A complex mixing of heavy- and light-hole states occurs when $k \neq 0$. From the difference of effective masses between heavy and light holes most of the holes should be heavy holes. There is a mass-reversal effect; the heavy-hole effective mass is heavy perpendicular to the p^- -type $\text{GaAs}/\text{Al}_x\text{Ga}_{1-x}\text{As}$ interface but is light parallel to the interface, while the light-hole effective mass is light perpendicular to the p^- -type $\text{GaAs}/\text{Al}_x\text{Ga}_{1-x}\text{As}$ interface but is heavy parallel to the interface.³⁷ Light-hole tunneling through $\text{Al}_x\text{Ga}_{1-x}\text{As}$ is favored since the tunneling probability depends exponentially on the hole mass normal to the barrier.

C. Sample uniformity

A characteristic feature of resonant or nonresonant tunneling through states in the barrier of a SIS capacitor is that samples that are otherwise identical have different patterns of structure in I - V curves. We have studied four p -type tunneling samples in details. C - V and I - V curves between 77 and 235 K have been used to show that the basic sample properties are nearly identical.

C - V curves for p -type $\text{Al}_x\text{Ga}_{1-x}\text{As}$ capacitors are nearly ideal, as is shown in Fig. 2(a). The solid line in Fig. 2(a) is an experimental C - V curve for sample A at 1 MHz and 77 K. The dotted curve is a C - V curve calculated using a classical model which has been used previously for n -type $\text{Al}_x\text{Ga}_{1-x}\text{As}$ capacitors.^{1,7} The parameters of the calculation are given on the figure. N_S is obtained from the experimental C - V curves. N_G and w_{cp} , the capacitance thickness, are obtained by comparing calculated and experimental C - V curves. ϵ_I is the dielectric constant of $\text{Al}_{0.5}\text{Ga}_{0.5}\text{As}$ used for calculations. The flat-band voltage, V_{FB} , for all the p -type $\text{Al}_{0.5}\text{Ga}_{0.5}\text{As}$ capacitors is 0.0 V. The model calculates V_{FB} as the difference between the Fermi levels of the p^+ -type GaAs gate and the p^- -type GaAs substrate. V_{SH} is the voltage by which the calculated C - V curve is shifted for it to coincide with the experimental C - V curve. The decrease in capacitance for $-0.6 \lesssim V_G \lesssim -0.1$ V is due to band bending in the p^+ -type GaAs gate. V_I , ψ_S , ψ_G , and the field across the insulator, F , are calculated as a function of V_G ; they are shown in Fig. 2(b) for sample A . As is the case for n -type $\text{Al}_x\text{Ga}_{1-x}\text{As}$ capacitors in accumulation, about $\frac{1}{4}$ of the

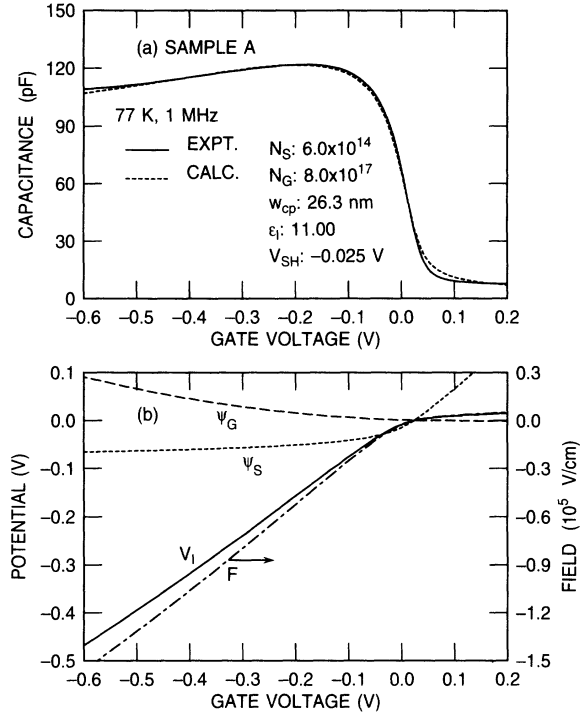


FIG. 2. (a) Experimental (solid) and calculated (dotted) capacitance curves for p -type $\text{Al}_x\text{Ga}_{1-x}\text{As}$ capacitor. Parameters are those used for calculated curve. Sample area: $4.0 \times 10^{-4} \text{ cm}^2$. (b) Dependence of ψ_S , ψ_G , V_I , and F on V_G , calculated from the theoretical C - V curve.

total applied voltage goes into band bending in substrate and gate.

Barrier heights for the samples are determined from the temperature dependence of I - V curves in the temperature range 100 to 235 K, where thermionic emission of holes over the $\text{GaAs}/\text{Al}_x\text{Ga}_{1-x}\text{As}$ barrier dominates the I - V curves.^{1,38-40} The current density due to thermionic emission, J , is given by

$$J = A^* T^2 \exp(-\phi_E/kT) \text{ A/cm}^2, \quad (1)$$

where A^* is the prefactor, ϕ_E is an effective barrier height, and T is the temperature. At 77 K, hole tunneling is the dominant conduction mechanism; currents are exponentially dependent on V_G for $V_G < 0.0$ V and they are almost unmeasurable for $V_G > 0.0$ V. Just as for n -type $\text{Al}_x\text{Ga}_{1-x}\text{As}$ capacitors, rectification occurs because the field across the $\text{Al}_x\text{Ga}_{1-x}\text{As}$ barrier is large when the lightly doped substrate of the $\text{Al}_x\text{Ga}_{1-x}\text{As}$ capacitor is in accumulation; it is very small when $V_G > 0$ V and the substrate is in depletion, as shown in Fig. 2(b). Currents for $V_G > 0$ V are too small to study hole tunneling into a depletion region as Alikacem *et al.* have done.^{14,15} Barrier heights are obtained from the slope of plots of $\ln(J/T^2)$ as a function of $1/T$ for T between 115 and 235 K, and A^* is obtained from the intercept. Figure 3(b) shows the effective barrier heights for sample A as a function of V_G . ϕ_G , measured when $V_G > 0$ V, is nearly constant. ϕ_S , the effective barrier height for emission of holes from the ac-

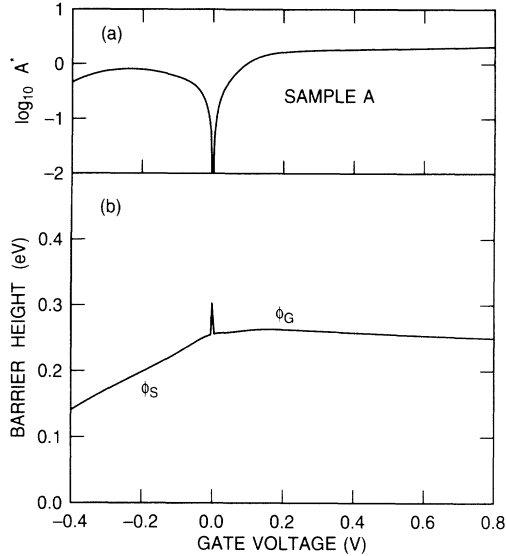


FIG. 3. (a) $\log_{10} A^*$ and (b) barrier height vs gate voltage, determined from thermionic emission analysis of I - V data. A^* is the prefactor for thermionic emission of holes over the barrier.

cumulation layer, decreases markedly as $|V_G|$ increases. This is primarily due to the increase in Fermi level E_F as the hole density increases; Schottky lowering of the barrier by the field may also contribute. For $V_G > 0$ V, $A^* \sim 2$ A/cm²-K² and is nearly constant, as shown in Fig. 3(a). For ideal thermionic emission of electrons into vacuum, A^* is Richardson's constant $A_0 = 120$ A/cm²-K². For ideal semiconductors $A^* \sim m_e A_0$, where m_e is the effective mass of the current carriers. For GaAs, there are both heavy holes of mass $m_{hh} = 0.5m_0$ and light holes of mass $m_{lh} = 0.09m_0$, where m_0 is the mass of the free electrons. If heavy holes were the dominant current carriers one would expect $A^* \sim 60$ A/cm²-K²; if light holes were dominant, $A^* \sim 10$ A/cm²-K². The experimental value $A^* \sim 2$ A/cm²-K² is very close to the measured value for electrons¹ and indicates that thermionic emission current is primarily due to light holes, even though they constitute only a small fraction of the total hole population in the valence band of GaAs.

Four samples have been studied in detail in the present work, all of which have Al_{0.5}Ga_{0.5}As dielectric layers. Samples *A*, *B*, and *D* have an area of 4.00×10^{-4} cm²; the area of sample *C* is 1.56×10^{-4} cm². Table I shows N_S , N_G , w_{cp} , A^* , and ϕ_G for the samples. They have essentially the same values for all these parameters. w_{cp} is ~ 26 nm and is larger than the nominal Al_{0.5}Ga_{0.5}As thickness of 20 nm. This occurs because C - V curves measure the thickness when the Al_xGa_{1-x}As capacitor is in accumulation. The centroid of the charge is not at the Al_{0.5}Ga_{0.5}As/GaAs interface but is displaced by ~ 3 nm by quantum effects. Similar effects are observed in n -type Al_xGa_{1-x}As capacitors.⁷ Values of ϕ_G are close to the value of the valence-band offset for the GaAs/Al_{0.5}Ga_{0.5}As interface, 0.275 eV.^{38,39} Except when comparing conduction in different samples, most

TABLE I. Properties of p -type Al_{0.5}Ga_{0.5}As capacitors. N_S is the substrate doping, N_G is the gate doping, w_{cp} is the Al_{0.5}Ga_{0.5}As thickness from C - V measurements, ϕ_G is the activation energy, and A^* is the prefactor for thermionic emission of holes.

Sample	N_S (10 ¹⁴ cm ⁻³)	N_G (10 ¹⁷ cm ⁻³)	w_{cp} (nm)	ϕ_G (eV)	$\log_{10} A^*$	A^*
<i>A</i>	6	8	26.3	0.263	0.2–0.3	1.6–2.0
<i>B</i>	6	8	26.3	0.259	0.1–0.2	1.3–1.6
<i>C</i>	6	7	27.1	0.266	0.2–0.3	1.6–2.0
<i>D</i>	6	7	25.7	0.266	0.1–0.2	1.3–1.6

results are given for sample *A* since it exhibits four true voltage-controlled negative resistance (VCNR) regions in its I - V characteristics at low temperature, and two regions that almost show VCNR.

III. RESULTS

A. Temperature dependence of I - V curves

A decrease in the fluctuations of conductance with increasing temperature is a characteristic feature of incoherent mesoscopic tunneling through impurity states in the barrier. Figure 4 shows I - V curves for sample *A* as a function of temperature between 40 and 2.4 K, and Fig. 5 shows $\ln(\sigma) = \ln(dJ/dV)$ for the same temperatures for $-0.5 \leq V_G \leq -0.1$ V. Data were taken at 0.001 V intervals to resolve the complex structure that occurs.

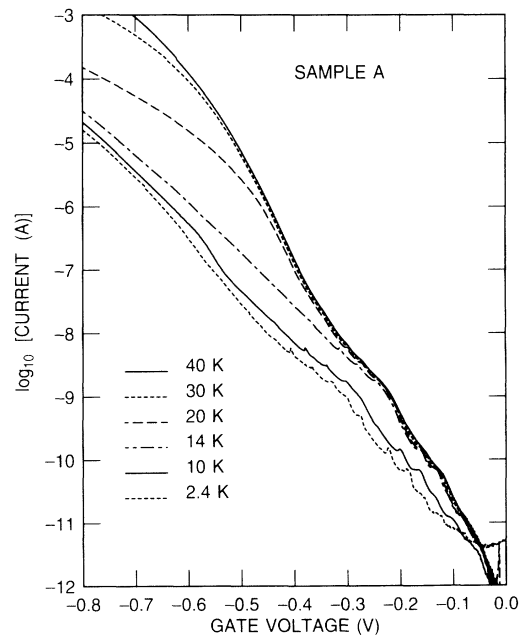


FIG. 4. Dependence of \log_{10} (current) on gate voltage for different temperatures for the p -type Al_xGa_{1-x}As capacitor. Note irregular structure in I - V curves at lowest temperatures.

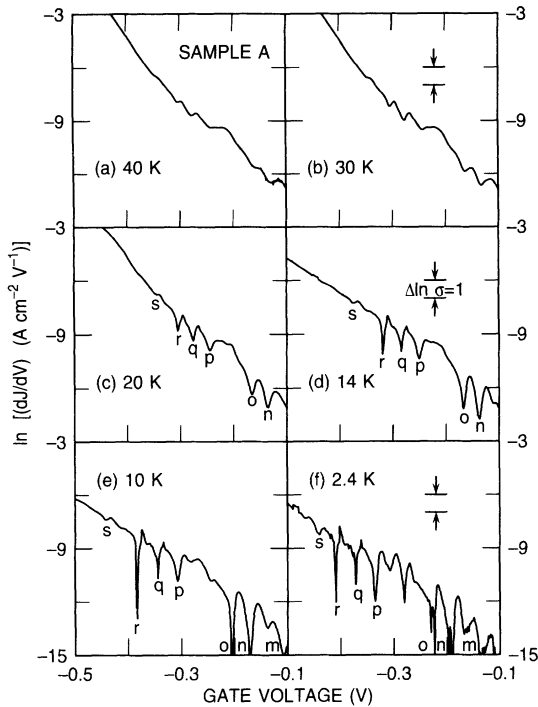


FIG. 5. Dependence of $\ln(dJ/dV) \equiv \ln(\sigma)$ on V_G for different temperatures for sample *A*. *m-s* identify reproducible minima.

Derivatives were calculated numerically from I - V curves. A limited voltage range is plotted in Fig. 5 since this is the region of pronounced structure in σ .

At 40 and 30 K, the I - V curves of samples *A* are relatively smooth although Fig. 5 shows there is definite structure in σ . By 10 K there are sharp negative resistance regions in the I - V curves. Figure 4 shows a problem with working with p -type $\text{Al}_x\text{Ga}_{1-x}\text{As}$ capacitors. From optical measurements the Be acceptor energy is 0.028 eV; from admittance measurements on these samples it is 0.020–0.023 eV.³² Holes freeze out in the temperature range from 30 to 10 K. The resistance of the 600-nm p -type GaAs substrate becomes large enough that there is a significant voltage drop across it. This first affects the higher current regions of the I - V curves and, below 20 K, shifts structure in I - V curves to higher voltages. This is clearly shown in Fig. 5 where five minima $n \cdots r$ have a characteristic structure of a doublet and a triplet. At 20 K their positions are not affected by acceptor freezeout; by 10 K the position of each is shifted to higher voltage but the pattern of structure remains. Two characteristics of the RR theory are that structure in I - V curves broadens and disappears as temperature increases, and that fluctuations in conductivity occur for which $\Delta \ln \sigma \sim 1$, due to conduction through specific states in the dielectric.^{27,31} Figure 5 shows that both these effects occur for sample *A*. The fluctuations in $\ln \sigma$ are of order 1, and are superimposed on the exponential dependence of current on voltage, which is due to direct tunneling of holes from the accumulation layer on p -type GaAs to the p -type GaAs gate.

An alternate way of presenting data which resolves

structure in greater detail is to plot $d(\ln J)/dV \equiv (1/J)dJ/dV$ versus gate voltage, as is done in Fig. 6. At 40 K a triplet and doublet structure is observed; such structure only disappears above ~ 70 K. Below 20 K fine structure develops in the derivatives which is completely reproducible. For example, the region between minima *o* and *p* has shoulders at 20 K but has two minima at 10 K and three minima in the derivative at 2.4 K. Another advantage of the derivative curve of Fig. 6 is that, for regions of VCNR, the value of the derivative is less than 0. The effect of acceptor freezeout on the position of minima in derivative curves is shown in Fig. 7, in which the voltage for different minima, V_{\min} , is plotted as a function of temperature. V_{\min} is constant within ± 0.001 V above 16 K; below 16 K, V_{\min} increases, with the voltage shift being larger the larger the current. The samples studied have relatively thick $\text{Al}_x\text{Ga}_{1-x}\text{As}$ barriers, ~ 20 nm, which results in low tunneling currents. This is advantageous for studying structure in I - V curves since $I < 10^{-8}$ A for the voltage range in which complex structure occurs in derivative curves. The shift in voltage of the structure with thinner dielectric barriers would be even larger because of larger currents. One reason for using sample *A* to illustrate data for all the samples is that its pattern of minima is relatively simple.

Two types of tunneling occur in $\text{Al}_x\text{Ga}_{1-x}\text{As}$ capacitors, direct tunneling, and Fowler-Nordheim (FN) tunneling. At low biases the barrier is trapezoidal and holes tunnel directly from one electrode to the other. At high biases the barrier becomes triangular; holes tunnel into

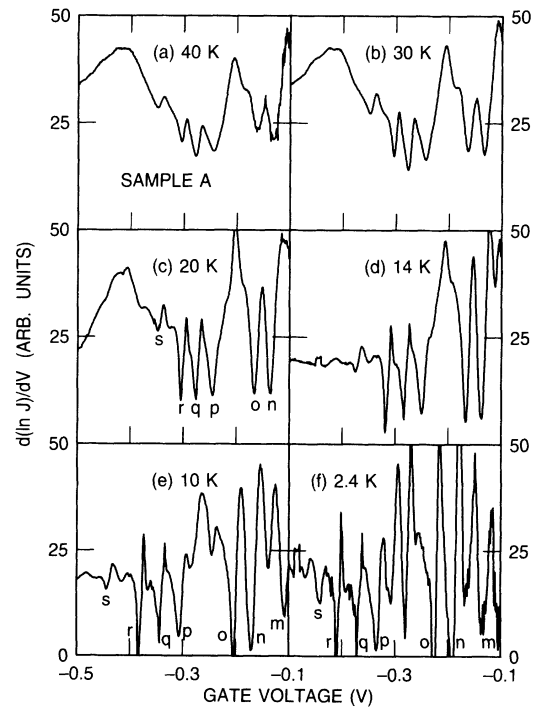


FIG. 6. Dependence of derivative curves, $d(\ln J)/dV \equiv (1/J)(dJ/dV)$, on V_G for different temperatures for sample *A*. *m-s* identify principal minima in derivative curves.

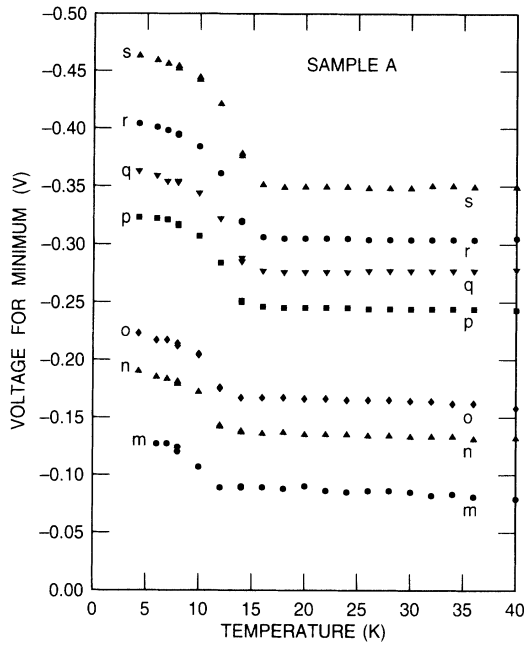


FIG. 7. Dependence of the voltage for different minima in derivative curves on temperature for sample *A*. Freezeout of acceptors in substrate shifts the position of minima between 15 and 5 K.

the valence band of $\text{Al}_x\text{Ga}_{1-x}\text{As}$ before reaching the p^+ -type GaAs gate. Such FN tunneling is illustrated in Fig. 1(a). The transition from one regime to the other occurs when V_I is greater than ϕ_G . From Fig. 2(b) this occurs when $V_G \lesssim -0.32$ V. The temperature-independent structure of Figs. 5 and 6 occurs in the direct tunneling regime. There is an increase in conductance of sample *A* when $|V_G| \gtrsim 0.32$ V, corresponding to the transition from direct tunneling to FN tunneling, but there is no structure corresponding to tunneling through states in the $\text{Al}_x\text{Ga}_{1-x}\text{As}$ dielectric for FN tunneling.

B. Sample variability

A characteristic feature of tunneling through “punctures” or impurity states in randomly nonuniform barriers is that the pattern of nonuniformity is sample specific; nominally identical samples show different structure in I - V curves and in plots of conductance versus voltage. Table I gives measured parameters for four samples that were grown on the same wafer. The reproducibility from sample to sample is very good. Figure 8 shows $\ln J$ (dotted) and $\ln(dJ/dV) \equiv \ln(\sigma)$ (solid) as a function of voltage for $-0.4 \leq V_G \leq 0.0$ V, the direct tunneling regime in which there is structure due to tunneling through states in the $\text{Al}_x\text{Ga}_{1-x}\text{As}$ barrier. The temperature is 18 K for each sample; the temperature is low enough that structure in conductance is well developed but is high enough that freezeout of the p^- -type GaAs substrate does not shift the position of the fluctuations. The current through all four samples depends exponentially on voltage in similar fashion, the thresholds for detectable current are about the same, and all four samples

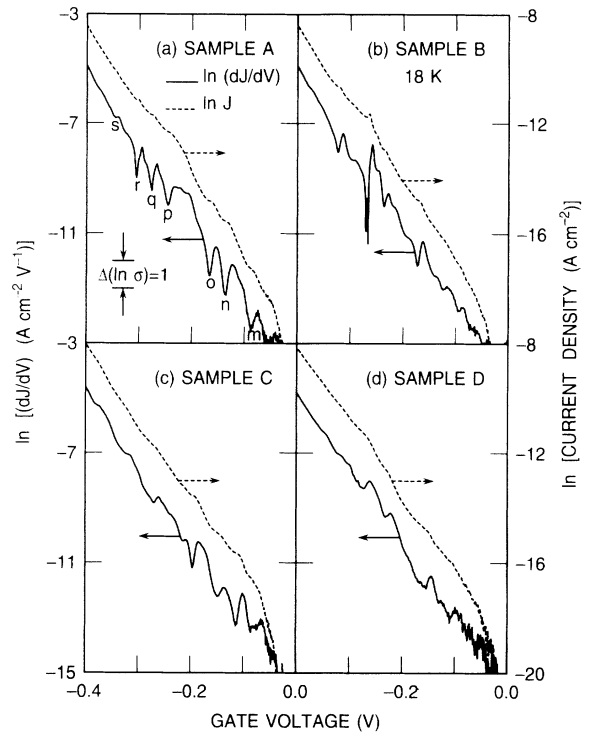


FIG. 8. Dependence of $\ln(J)$ (dotted) and of $\ln(dJ/dV) \equiv \ln(\sigma)$ (solid) on V_G for different p -type $\text{Al}_x\text{Ga}_{1-x}\text{As}$ capacitors with nominally identical properties. $T = 18$ K for all samples.

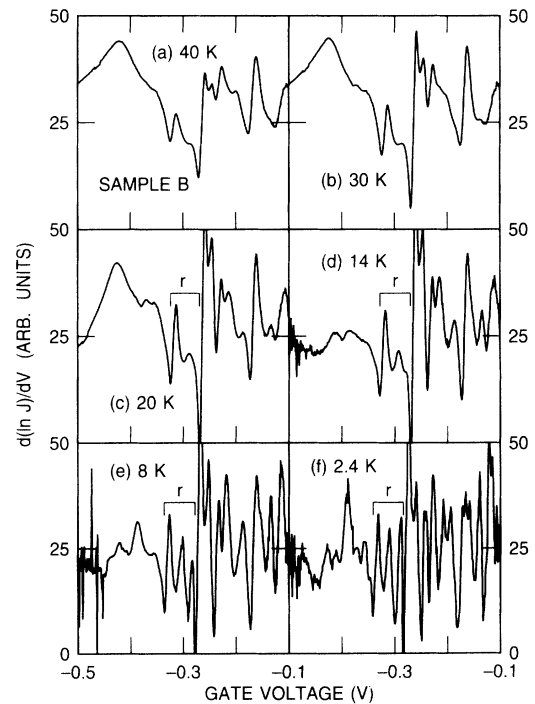


FIG. 9. Dependence of derivative curves, $d(\ln J)/dV$, on V_G for different temperatures for sample *B*. *r* identifies a voltage region where complex structure develops as temperature decreases.

have fluctuations $\Delta \ln \sigma \sim 1$, as shown by horizontal bars in Fig. 8(a). Just as with sample *A*, I - V curves and their derivatives are reproducible to ± 0.001 V for all the samples over the temperature range from 1.7 to 70 K. In detail, the voltages for maxima and minima in conductance differ markedly for the four samples.

Sample *B* illustrates the complexity of the structure that can develop in derivative curves as temperature is lowered. Figure 9 shows $d(\ln J)/dV$ versus gate voltage for different temperatures for sample *B*. At 20 K and lower there is a VCNR minimum at $V_G = -0.27$ V which is the only VCNR region for the sample. In the region *r* there is a doublet in the maxima of the derivative. At 14 K the doublet develops a shoulder which becomes a well-defined triplet at 8 K and lower temperatures. The two maxima for $-0.27 \lesssim V_G \lesssim -0.22$ V are doublets at 30 K and lower, and at 2.4 K there are four doublets in the maxima of the derivatives between -0.15 and -0.28 V. Thus each sample has a characteristic pattern of fluctuations in derivative curves with temperature-dependent fine structure, but the pattern varies from sample to sample.

C. Magnetic fields

Fluctuations in the conductance of mesoscopic systems due to conduction through ‘‘punctures’’ or states in a barrier do not depend on the interference of electrons that take different paths through a sample. Consequently there should be no effect of magnetic field on the conductance fluctuations of a sample that exhibits incoherent mesoscopic conduction through single deep states in the barrier. The magnetic field can change fluctuations because of Zeeman effects or spin splitting in impurity states.

Figure 10 shows $d(\ln J)/dV$ as a function of V_G for different values of magnetic field B perpendicular to sample *A*. Figure 10(c) identifies minima in the derivative, *m* through *r*, which correspond to the same minima in Figs. 5 and 6. (Note that the voltage scale differs for the figures.) Values of V_G for these minima, as a function of perpendicular B , are plotted as solid points in Fig. 11(b). There is no significant change of V_{\min} with B , which is consistent with the structure in I - V curves being due to resonant tunneling through states in $\text{Al}_x\text{Ga}_{1-x}\text{As}$ barrier.

The structure in derivative curves in Fig. 10 is substantially more complex than in the curves of Fig. 6. Primarily the increase in complexity is due to lowering the temperature. In particular, structure develops between minima *o* and *p* as temperature is reduced. However, superimposed on the structure due to tunneling through states in the barrier is structure which depends on magnetic field. V_G for minima labeled α and β in Figs. 10(c)–10(f) are proportional to B as is shown in Fig. 11(b). For $-0.4 \lesssim V_G \lesssim -0.1$ V, changes in the derivative due to α and β can be identified but are masked by structure due to incoherent mesoscopic tunneling. Minima α and β are clearly shown for $-0.7 \lesssim V_G \lesssim -0.4$ V, where structure due to tunneling through states in $\text{Al}_x\text{Ga}_{1-x}\text{As}$ does not dominate derivative curves.

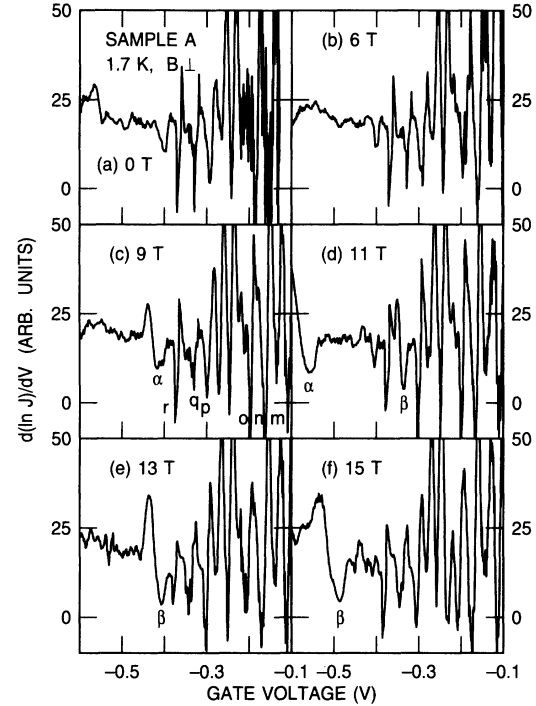


FIG. 10. Dependence of derivative curves, $d(\ln J)/dV$, on V_G for different perpendicular magnetic fields for sample *A*. *m*-*s* identify reproducible minima, α and β identify minima whose positions are proportional to B .

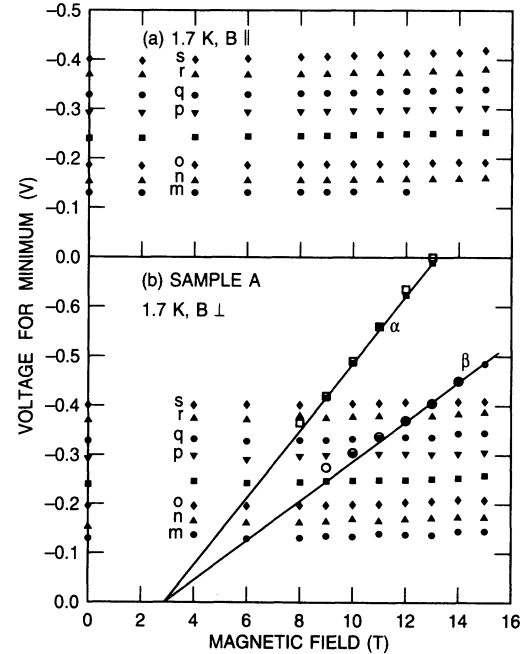


FIG. 11. Dependence of the voltage for different minima in derivative curves of sample *A* on magnetic field: (a) for B parallel to sample, and (b) for B perpendicular to sample. Open points and large solid points in (b) are obtained from ac conductance-voltage curves.

Hole tunneling in p -type $\text{Al}_x\text{Ga}_{1-x}\text{As}$ capacitors is from an accumulation layer, as shown schematically in Fig. 1(a). Holes in an accumulation layer occur in subbands, each of which has a minimum energy which is determined by the effective mass of the carriers.⁴¹ For GaAs the lowest subband, with energy E_0 , is a heavy-hole band; its energy is determined by the effective hole mass perpendicular to the p -type GaAs/ $\text{Al}_x\text{Ga}_{1-x}\text{As}$ interface. There is a mass-reversal effect in a two-dimensional hole gas on GaAs; holes that are heavy holes perpendicular to the GaAs/ $\text{Al}_x\text{Ga}_{1-x}\text{As}$ interface are light holes parallel to the interface, and vice versa.³⁷ In addition, when $k \neq 0$, there is a complex mixing of light- and heavy-hole states; similar complex mixing of hole states also occurs in high magnetic fields.⁴²

In a perpendicular magnetic field each of the hole subbands forms Landau levels.⁴¹ For a parabolic energy band, if E_{i0} is the lowest energy of a particular subband at 0 T, in a magnetic field B , $E_i = E_{i0} + (N + 1/2)\hbar\omega_i$. $\hbar\omega_i = qB\hbar/m_i$ is the cyclotron energy for holes which have an effective mass m_i , and $N = 0, 1, \dots$ is the Landau-level index. The effective mass that determines $\hbar\omega_i$ is the effective mass parallel to the p -type GaAs/ $\text{Al}_x\text{Ga}_{1-x}\text{As}$ interface. Observation of magnetic-field-dependent minima in Fig. 10 is consistent with a light-hole mass for holes parallel to the interface; it does not tell what the mass is.

Structure in derivative curves such as those in Fig. 10 due to Landau levels is easily resolved for $|V_G| \gtrsim 0.4$ V since there is no structure due to tunneling through states in the $\text{Al}_x\text{Ga}_{1-x}\text{As}$ barrier. For $-0.4 \lesssim V_G \lesssim 0.0$ V, because of the complex structure at all values of B , it is much more difficult to track structure in I - V curves due to the effect of magnetic field. ac conductance measurements can simplify their identification. Capacitance-voltage curves of p -type $\text{Al}_x\text{Ga}_{1-x}\text{As}$ capacitors, such as in Fig. 2(a), are measured with an LCR meter which measures the parallel capacitance, C_p , and ac conductance, G_p , of the heterostructure.³² In studies of magnetotunneling in n -type $\text{Al}_x\text{Ga}_{1-x}\text{As}$ capacitors it has been shown that structure occurs in both C_p and G_p curves that reflects minima in the density of states in an accumulation layer due to the occurrence of Landau levels.^{8,9} At 1.7 K Be acceptors in the p -type GaAs substrate are frozen out, which results in a very high series resistance. This causes C_p measured in accumulation to have a constant small value. The magnitude of G_p is also reduced by series resistance but it shows well-resolved Landau-level structure. In Fig. 12, conductance-voltage curves at 10 kHz are shown for sample A at different perpendicular magnetic fields. The dotted curve in Fig. 12(b) shows a typical C - V curve and illustrates the suppression of C_p by series resistance. G - V curves do not show the complex structure of I - V curves but have minima, α and β , at values of V_G that are linearly proportional to B . The open circles, or large solid circles, in Fig. 1(b) show the α minima and the large open squares show the β minima; they agree closely with magnetic-field-dependent minima in I - V curves. For G - V curves, α peaks are not resolved for $B < 8$ T; β peaks are unresolved for $B < 9$ T. A third

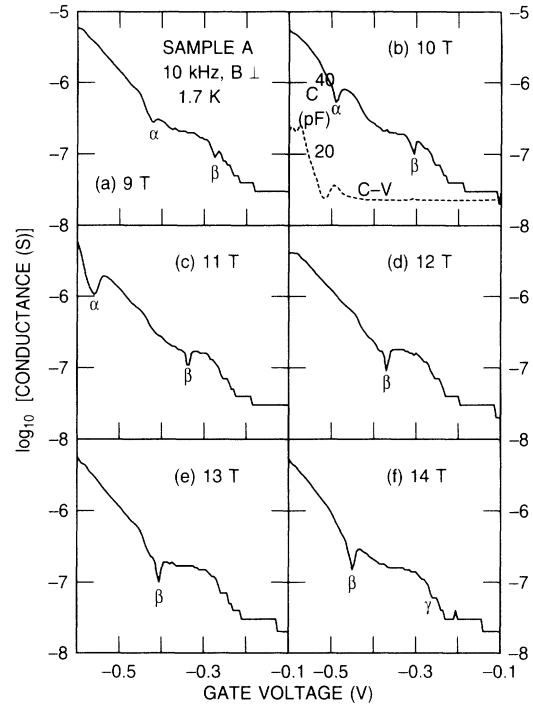


FIG. 12. Dependence of ac conductance at 10 kHz on V_G for sample A in different perpendicular magnetic fields, α , β , and γ are minima whose position is proportional to B . Dotted curve in (b) shows a 10-kHz C - V curve at 1.7 K and 10 T.

minimum γ appears in Fig. 12(f) but is not well resolved.

Studies of magnetocapacitance and magnetotunneling curves for n -type GaAs capacitors in a perpendicular magnetic field have shown that structure in C - V , G - V , or I - V curves depends on changes in the density of states in the accumulation layer at the GaAs/ $\text{Al}_x\text{Ga}_{1-x}\text{As}$ interface due to formation of Landau levels.^{8,9} C - V and G - V curves reflect changes in the density of states due to filling or emptying of states from the back contact through the lightly doped substrate. I - V curves reflect the effect of the density of states on tunneling through the $\text{Al}_x\text{Ga}_{1-x}\text{As}$ barrier. The curves of Figs. 10 and 12 are an extreme example of this difference. In Fig. 10 structure due to tunneling from a varying density of states in the accumulation layer is superimposed on a remarkably complex structure due to tunneling through states in the $\text{Al}_x\text{Ga}_{1-x}\text{As}$ barrier. In Fig. 12, G - V curves at 10 kHz, show none of the complex structure of the I - V curves but show changes in the density of states due to the formation of Landau levels.

When measuring I - V curves, increasing $|V_G|$ increases N_H , the number of holes in the accumulation layer. The field at the p -type GaAs/ $\text{Al}_x\text{Ga}_{1-x}\text{As}$ interface increases, ψ_S increases, and $E_F - E_0$ increases as N_H increases. If a perpendicular B is constant the hole Fermi level moves through a sequence of Landau levels which is not necessarily linear in B due to the complex mixing of light-hole and heavy-hole states. The dependence of N_H on V_G can be estimated by integrating C - V curves, as is shown by the solid curve in Fig. 13(a), where N_H versus

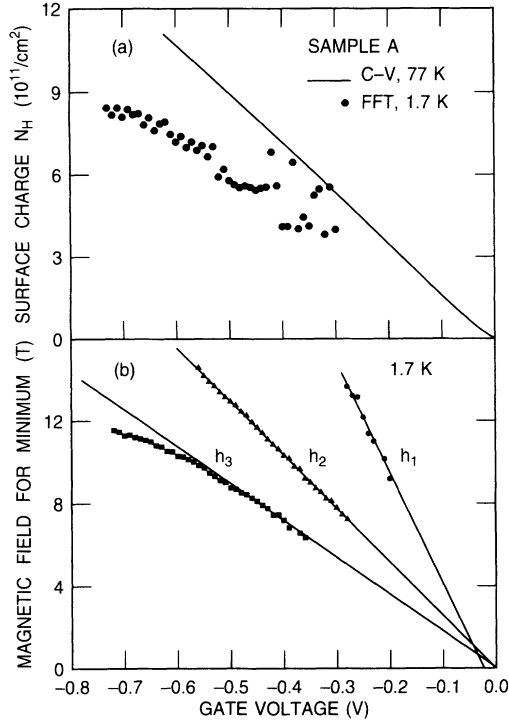


FIG. 13. (a) Dependence of hole concentration in accumulation layer of sample *A* on V_G . Solid line from integrating C - V curve at 1 MHz and 77 K; solid points from Fourier analysis of I - V - B curves. (b) Dependence of magnetic field for minima of I - V - B curves on V_G .

V_G , derived from the C - V curve of sample *A* at 77 K and 1 MHz is given. The curve at 77 K is used because series resistance of the p^- -type GaAs substrate due to acceptor freezeout at lower temperature can reduce the magnitude of capacitance and distort N_H . A complementary measurement is to measure current at constant V_G as B is changed, an I - V - B curve. Holding V_G constant means that N_H , ψ_S , and E_F are nearly constant. Figure 14 shows the ratio $I(B)/I(0)$ at constant V_G as a function of B for several values of V_G , where $I(0)$ is the current at 0 T. The curves of Fig. 14 are shifted with respect to each other but all are plotted on the same ordinate scale. Horizontal lines correspond to $I(B)/I(0)=1.0$. All curves show a decrease in $I(B)/I(0)$ as B increases. Minima corresponding to three successive levels occur. As typified by Fig. 14(a), for $-0.20 \lesssim V_G \lesssim -0.10$ V there is no structure in I - V - B curves that depends on B . For $-0.28 \lesssim V_G \lesssim -0.20$ V the value of B for minimum h_1 is proportional to V_G . The minimum h_2 can be resolved for $-0.57 \lesssim V_G \lesssim -0.28$ V, and for $V_G \lesssim -0.36$ V h_3 moves to higher values of B . B - V_G plots for h_1 , h_2 , and h_3 are shown in Fig. 13(b); h_3 corresponds approximately to α in Fig. 11(b), h_2 corresponds to β , and h_1 corresponds to γ in Fig. 12(f), which can be resolved in G - V plots but not in I - V plots. The lines in Fig. 13(b) are least-square lines drawn through the lowest voltage points. Although h_1 and h_2 are linear in plots of B_{\min} versus V_G , there is pronounced curvature for minimum

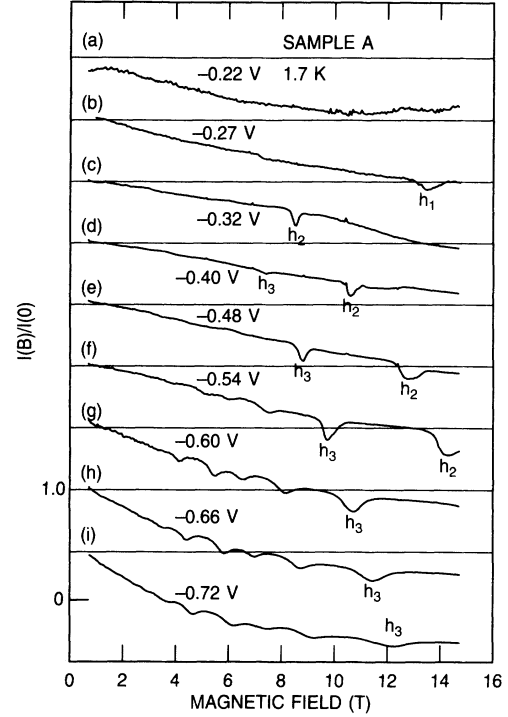


FIG. 14. $I(B)/I(0)$ as a function of perpendicular magnetic field for different fixed values of gate voltage. h_1 , h_2 , and h_3 show minima whose position is proportional to V_G and B . Curves are shifted vertically for clarity; horizontal lines are at $I(B)/I(0)=1.0$.

h_3 . The minima h_1 , h_2 and h_3 appear to be due to separate subbands in the accumulation layer rather than to Landau levels of a heavy-hole band.

In addition to minima h_1 , h_2 , and h_3 there are minima in Figs. 14(f)–14(i) for $B \gtrsim 3$ T. Similar structure is observed for I - V - B and C - V - B curves of n -type $\text{Al}_x\text{Ga}_{1-x}\text{As}$ capacitors.^{8,9} If plotted as a function of Landau-level index N , the spacing of the minima is proportional to $1/B$. For n -type GaAs capacitors, they are due to the passage of successive minima of Landau levels through the Fermi level of the two-dimensional electron gas of the accumulation layer. Fast Fourier transform (FFT) analysis of I - V - B and C - V - B curves as a function of $1/B$ has been used to determine the surface concentration of electrons in the accumulation layer of n -type $\text{Al}_x\text{Ga}_{1-x}\text{As}$ capacitors.⁹ By analogy, as N_H increases due to increasing V_G , the Fermi level in the accumulation layer moves from a heavy-hole subband into a light-hole subband. Landau levels are not resolved in the heavy-hole band but are in the light-hole subband, with a consequent modulation of the density of states at the Fermi level. This in turn modulates the tunneling current with a period proportional to $1/B$. The results of a similar FFT analysis of the I - V - B curves of Fig. 14 are shown by the solid circles in Fig. 13(a), which plots N_H as a function of V_G . Minima cannot be resolved for $|V_G| \lesssim 0.3$ V. The solid curve gives N_H versus voltage from integrating a C - V curve at 77 K. For electrons, such a curve gives

N_H at a given voltage that is $\sim 10\%$ less than derived from FFT analysis of I - V - B or C - V - B data; however, all electrons have nearly the same effective mass. For holes, Fig. 13(a) suggests that about $\frac{2}{3}$ of the holes act as light holes when $N_H \gtrsim 5 \times 10^{11} \text{ cm}^{-2}$; the rest have heavy mass and their presence does not produce structure in I - V - B curves which is proportional to $1/B$. Alikacem *et al.* have made similar measurements of the dependence of hole density on bias.¹⁴

If the magnetic field is parallel to the p^- -type GaAs/ $\text{Al}_x\text{Ga}_{1-x}\text{As}$ interface, Landau levels do not form in the accumulation layer on the substrate. If conduction is through states in the $\text{Al}_x\text{Ga}_{1-x}\text{As}$ layer, parallel fields should not affect structure in I - V curves. In Fig. 11(a) the values of V_G for different minima in the derivative curve are given as a function of parallel magnetic field. The values of V_{\min} are constant, just as they are in perpendicular magnetic field. One of the most striking features of hole tunneling is the occurrence of VCNR regions in the I - V curves. Larkin and Matveev⁴³ have suggested that negative differential conductance can occur if pairs of impurities are involved in a conduction path. In such a case a parallel magnetic field could affect incoherent mesoscopic tunneling by changing the phase of holes as they tunnel from one impurity of the pair to the other. Both sample *A* and sample *B* have VCNR regions in their I - V characteristics. For parallel magnetic fields $B \gtrsim 11 \text{ T}$ the conductance does not drop to negative values; VCNR in the I - V curves is eliminated for both samples.

IV. DISCUSSION

Four features are characteristic of incoherent mesoscopic tunneling through transmittancy fluctuations or "punctures" in a tunnel barrier. First, I - V characteristics are stable and reproducible for a given sample but conductivity varies between nominally identical samples. Second, the conductance of different samples fluctuates around an average value with fluctuations in $\ln\sigma$ of the order of 1. Third, increasing temperature broadens fluctuations in conductance and eventually causes them to disappear; and fourth, conductance fluctuations are independent of magnetic field. Hole tunneling from an accumulation layer in p -type $\text{Al}_x\text{Ga}_{1-x}\text{As}$ capacitors exhibits all these characteristics. From the data, the principal conduction mechanism for $T \lesssim 77 \text{ K}$ is tunneling of light holes through the $\text{Al}_x\text{Ga}_{1-x}\text{As}$ barrier, and the complexity of the I - V curves is due to tunneling of holes through a small number of states that are distributed randomly in position and energy in the $\text{Al}_x\text{Ga}_{1-x}\text{As}$ barrier.

The origin of the states in the $\text{Al}_x\text{Ga}_{1-x}\text{As}$ barrier is uncertain but the most likely source is Be acceptors that have diffused in from the p^+ -type GaAs gate during sample growth. Many measurements have been made on tunneling in n -type $\text{Al}_x\text{Ga}_{1-x}\text{As}$ capacitors; while there is extensive structure in magnetotunneling curves due to Landau levels in an accumulation layer or to Landau states in the n^+ -type GaAs gate, no structure similar to that which occurs in hole tunneling has been observed. Substitutional Be is an acceptor in both GaAs and

$\text{Al}_x\text{Ga}_{1-x}\text{As}$. From optical measurements the hole binding energy is 0.028 eV in GaAs and 0.049 eV in $\text{Al}_{0.5}\text{Ga}_{0.5}\text{As}$.⁴⁴ The temperature region for the disappearance of fluctuations in conductance of p -type $\text{Al}_x\text{Ga}_{1-x}\text{As}$ capacitors reaches up to 70 K, which is consistent with the hole binding energy in $\text{Al}_{0.5}\text{Ga}_{0.5}\text{As}$. In addition, Be diffusion in GaAs and $\text{Al}_x\text{Ga}_{1-x}\text{As}$ is anomalously rapid during MBE growth of heavily Be-doped heterostructures.⁴⁵⁻⁴⁸ Diffusion by interstitial Be can give rapid in-diffusion of Be from the p^+ -type GaAs gate region into $\text{Al}_x\text{Ga}_{1-x}\text{As}$. The extent of Be diffusion into $\text{Al}_x\text{Ga}_{1-x}\text{As}$ is not enough to destroy its effectiveness as a tunnel barrier but is sufficient to provide randomly distributed impurity states in the barrier through which tunneling can occur since only a small number of states are needed in the barrier.

There is a difficulty in having a shallow acceptor Be as the origin of impurity states in the $\text{Al}_{0.5}\text{Ga}_{0.5}\text{As}$ barrier. Barrier states affect tunneling current most strongly when they are located in the middle of the barrier and have an energy equal to the Fermi level of the accumulation layer.²² In Fig. 1(a), E_A shows the approximate energy position of the shallow acceptor in $\text{Al}_{0.5}\text{Ga}_{0.5}\text{As}$. If conduction is through shallow states they should only become a conduction channel when $V_I \gtrsim \phi_G - E_A$, just before the onset of FN tunneling. From Fig. 2(b), this corresponds to $|V_G| \gtrsim 0.27 \text{ V}$. However, complex structure is observed for $|V_G| \gtrsim 0.100 \text{ V}$, and no structure is observed in the FN tunneling regime. If Be is responsible for barrier states it needs to introduce deep states as well as shallow states in the forbidden gap. It may be possible to test whether Be acceptors in $\text{Al}_x\text{Ga}_{1-x}\text{As}$ are the source of structure in tunneling by deliberately doping the barrier during growth.

There are two papers on hole tunneling in a similar Be-doped p -type $\text{Al}_x\text{Ga}_{1-x}\text{As}$ capacitor. Alikacem *et al.*^{14,15} have used a structure with a thinner $\text{Al}_{0.4}\text{Ga}_{0.6}\text{As}$ dielectric layer, 12.7 nm, compared to a 20-nm $\text{Al}_{0.5}\text{Ga}_{0.5}\text{As}$ barrier in the present work. For $V_G > 0 \text{ V}$, holes tunnel from the p^+ -type GaAs gate into a GaAs depletion region. For $V_G \gtrsim 0.4 \text{ V}$ they find a sequence of peaks in d^2I/dV^2 with a spacing of $39 \pm 2 \text{ mV}$ which they attribute to the interaction of LO phonons with holes that tunnel through the barrier. They compare their results to structure in I - V curves of n -type $\text{Al}_x\text{Ga}_{1-x}\text{As}$ capacitors due to electrons interacting with LO phonons after tunneling into an n^- -type GaAs depletion region.²⁻⁴ For electrons, a sequence of peaks with 36-mV spacing is observed for $-1.2 \lesssim V_G \lesssim -0.040 \text{ V}$ in both I - V and C - V curves. No other structure is observed. For hole tunneling and for $0.0 \lesssim V_G \lesssim 0.4 \text{ V}$, Alikacem *et al.* report complex structure in d^2I/dV^2 which disappears above about 50 K. The structure is similar to that observed here, suggesting that conduction through impurity states in the barrier is superimposed on current due to direct tunneling of holes. They do not give derivative spectra of I - V curves for tunneling from an accumulation layer. It is possible that their 39-mV structure is due to tunneling through states in the $\text{Al}_x\text{Ga}_{1-x}\text{As}$ barrier rather than to interaction of holes with LO phonons. Studies

of hole tunneling in double-barrier^{49,50} or triple-barrier heterostructures⁵¹ show VCNR in I - V characteristics but do not show structure that is clearly identified with hole tunneling through impurity states in the barrier.

In conclusion, complex structure is observed in I - V curves of p -type $\text{Al}_x\text{Ga}_{1-x}\text{As}$ capacitors. The structure is superimposed on direct tunneling of holes from an accumulation layer through an $\text{Al}_x\text{Ga}_{1-x}\text{As}$ barrier. It is consistent with what is expected for incoherent mesoscopic tunneling of carrier through a few "punctures" or impurity states in the barrier that have an exponential spread in transmittance, as discussed by Raikh and Ruzin.²⁷ p -type $\text{Al}_x\text{Ga}_{1-x}\text{As}$ capacitors are essentially an ideal system for studying mesoscopic tunneling through states in the barrier. Substrate, gate, and barrier regions

are lattice-matched single crystals. Barrier heights can be varied by varying the Al content of $\text{Al}_x\text{Ga}_{1-x}\text{As}$, and the density and distribution of impurity states may be varied by changing growth conditions of the heterostructures.

ACKNOWLEDGMENTS

The p -type $\text{Al}_x\text{Ga}_{1-x}\text{As}$ samples were grown by H. Meier and capacitors were processed by K. Seo. The structures they produced were essential for this work. Magnetic-field measurements were made through the courtesy of F. Fang. I have benefited from conversations with M. Heiblum, F. Stern, A. B. Fowler, E. E. Mendez, and W. T. Masselink.

- ¹T. W. Hickmott, P. M. Solomon, R. Fischer, and H. Morkoç, *J. Appl. Phys.* **57**, 2844 (1985).
- ²T. W. Hickmott, P. M. Solomon, F. F. Fang, F. Stern, R. Fischer, and H. Morkoç, *Phys. Rev. Lett.* **52**, 2053 (1984).
- ³T. W. Hickmott, P. M. Solomon, F. F. Fang, R. Fischer, and H. Morkoç, in *Proceedings of the 17th International Conference on the Physics of Semiconductors, San Francisco, 1984*, edited by J. D. Chadi and W. A. Harrison (Springer-Verlag, New York, 1985), p. 417.
- ⁴L. Eaves, P. S. S. Guimarães, B. R. Snell, D. C. Taylor, and K. E. Singer, *Phys. Rev. Lett.* **53**, 262 (1985).
- ⁵For a review, see J. P. Leburton, *The Physics of the Two-Dimensional Electron Gas*, edited by J. T. DeVreese and F. M. Peeters (Plenum, New York, 1987), p. 227.
- ⁶T. W. Hickmott, P. M. Solomon, R. Fischer, and H. Morkoç, *Appl. Phys. Lett.* **44**, 90 (1984).
- ⁷T. W. Hickmott, *Phys. Rev. B* **40**, 11 683 (1989).
- ⁸T. W. Hickmott, *Phys. Rev. B* **32**, 6531 (1985).
- ⁹T. W. Hickmott, *Phys. Rev. B* **39**, 5198 (1989).
- ¹⁰T. W. Hickmott, *Solid State Commun.* **63**, 371 (1987).
- ¹¹B. R. Snell, K. S. Chan, F. W. Sheard, L. Eaves, G. A. Toombs, D. K. Maude, J. C. Portal, S. J. Bass, P. Claxton, G. Hill, and M. A. Pate, *Phys. Rev. Lett.* **59**, 2806 (1987).
- ¹²T. W. Hickmott, *Phys. Rev. B* **44**, 12 880 (1991).
- ¹³T. W. Hickmott, *Solid State Commun.* **76**, 315 (1990).
- ¹⁴M. Alikacem, D. K. Maude, M. Henini, L. Eaves, G. Hill, and M. A. Pate, *Semicond. Sci. Technol.* **7**, B446 (1992).
- ¹⁵M. Alikacem, D. K. Maude, L. Eaves, M. Henini, G. Hill, and M. A. Pate, *App. Phys. Lett.* **59**, 3124 (1991).
- ¹⁶C. B. Duke, *Tunneling in Solids* (Academic, New York, 1969), p. 135.
- ¹⁷J. Lambe and R. C. Jaklevic, *Phys. Rev.* **165**, 821 (1968).
- ¹⁸R. H. Koch and A. Hartstein, *Phys. Rev. Lett.* **54**, 1848 (1985).
- ¹⁹S. J. Bending and M. R. Beasley, *Phys. Rev. Lett.* **55**, 324 (1985).
- ²⁰M. Naito and M. R. Beasley, *Phys. Rev. B* **35**, 2548 (1987).
- ²¹A. B. Fowler, G. L. Timp, J. J. Wainer, and R. A. Webb, *Phys. Rev. Lett.* **57**, 138 (1986).
- ²²A. B. Fowler, J. J. Wainer and R. A. Webb, *IBM J. Res. Dev.* **32**, 138 (1986).
- ²³T. E. Kopley, P. L. McEuen, and R. G. Wheeler, *Phys. Rev. Lett.* **61**, (1988).
- ²⁴D. Popovic, A. B. Fowler, S. Washburn, and P. J. Stiles, *Phys. Rev. B* **42**, 1759 (1990).
- ²⁵D. Popovic, A. B. Fowler, and S. Washburn, *Phys. Rev. Lett.* **67**, 2870 (1991).
- ²⁶G. Dearnaley, A. M. Stoneham, and D. V. Morgan, *Rep. Prog. Phys.* **33**, 1129 (1970).
- ²⁷M. E. Raikh and I. M. Ruzin, in *Mesoscopic Phenomena in Solids*, edited by B. L. Altshuler, P. A. Lee, and R. A. Webb (North-Holland, Amsterdam, 1991), p. 315.
- ²⁸RR use the term "punctures" or "perforations" for regions of high transmittancy. This has the implication of pinholes or thin spots in the barrier which is not the case for p -type $\text{Al}_x\text{Ga}_{1-x}\text{As}$ capacitors. Consequently, the terms "impurity states" or "states" are used interchangeably with "punctures."
- ²⁹A. V. Chaplik and M. V. Entin, *Zh. Eksp. Teor. Fiz.* **67**, 208 (1974) [*Sov. Phys. JETP* **40**, 106 (1975)].
- ³⁰I. M. Lifshitz and V. Ya. Kirpichenkov, *Zh. Eksp. Teor. Fiz.* **77**, 989 (1979) [*Sov. Phys. JETP* **50**, 499 (1979)].
- ³¹M. E. Raikh and I. M. Ruzin, *Zh. Eksp. Teor. Fiz.* **92**, 2257 (1987) [*Sov. Phys. JETP* **65**, 1273 (1987)].
- ³²T. W. Hickmott, *Phys. Rev. B* **44**, 13 487 (1991).
- ³³E. Bangert and G. Landwehr, *Superlatt. Microstruct.* **1**, 363 (1985).
- ³⁴T. Ando, *J. Phys. Soc. Jpn.* **54**, 1528 (1985).
- ³⁵M. Altarelli, in *Proceedings of Les Houches Winter School, Heterojunctions and Semiconductor Superlattices*, edited by G. Allan, G. Bastard, N. Boccara, M. Lannoo, and M. Voos (Springer, New York, 1986), p. 12.
- ³⁶D. A. Broido and L. J. Sham, *Phys. Rev. B* **31**, 888 (1985).
- ³⁷G. Bastard, *Wave Mechanics Applied to Semiconductor Heterostructures* (Les Editions de Physique, Paris, 1988), p. 105.
- ³⁸J. Batey and S. L. Wright, *J. Appl. Phys.* **59**, 200 (1986).
- ³⁹J. M. Langer, C. Delerue, M. Lannoo, and H. Heinrich, *Phys. Rev. B* **38**, 7723 (1988).
- ⁴⁰M. Rossmannith, K. Leo, and K. von Klitzing, *J. Appl. Phys.* **69**, 3641 (1991).
- ⁴¹T. Ando, A. B. Fowler, and F. Stern, *Rev. Mod. Phys.* **54**, 437 (1982).
- ⁴²U. Ekenberg and M. Altarelli, *Phys. Rev. B* **32**, 3712 (1985).
- ⁴³A. I. Larkin and K. A. Matveev, *Zh. Eksp. Teor. Fiz.* **93**, 1030 (1987) [*Sov. Phys. JETP* **66**, 580 (1987)].
- ⁴⁴V. Swaminathan, J. L. Zilko, W. T. Tsang, and W. R. Wagner, *J. Appl. Phys.* **53**, 5163 (1982).
- ⁴⁵D. L. Miller and P. M. Asbeck, *J. Appl. Phys.* **57**, 1816 (1985).

- ⁴⁶P. Enquist, G. W. Wicks, L. F. Eastman, and C. Hitzman, J. Appl. Phys. **58**, 4130 (1985).
- ⁴⁷R. L. S. Devine, C. T. Foxon, B. A. Joyce, J. B. Clegg, and J. P. Gowers, Appl. Phys. A **44**, 195 (1987).
- ⁴⁸S. Yu, T. Y. Tan, and U. Gösele, J. Appl. Phys. **69**, 3547 (1991).
- ⁴⁹E. E. Mendez, W. I. Wang, B. Ricco, and L. Esaki, Appl. Phys. Lett. **47**, 415 (1985).
- ⁵⁰R. K. Hayden, D. K. Maude, L. Eaves, E. C. Valadares, M. Henini, F. W. Sheard, O. H. Hughes, J. C. Portal, and L. Cury, Phys. Rev. Lett. **66**, 1749 (1991).
- ⁵¹T. Nakagawa, T. Fujita, Y. Matsumoto, T. Kojima, and K. Ohta, Appl. Phys Lett. **50**, 974 (1987).